Article

SOURCE DATA

EMBO reports

Epigenetic regulator Stuxnet modulates octopamine effect on sleep through a Stuxnet-Polycomb-Octβ2R cascade

Zhangwu Zhao[1,†], Xianguo Zhao[1,†], Tao He[2], Xiaoyu Wu[1], Pengfei Lv[1], Alan J Zhu[2] & Juan Du[1,*]

Abstract

Sleep homeostasis is crucial for sleep regulation. The role of epigenetic regulation in sleep homeostasis is unestablished. Previous studies showed that octopamine is important for sleep homeostasis. However, the regulatory mechanism of octopamine reception in sleep is unknown. In this study, we identify an epigenetic regulatory cascade (Stuxnet-Polycomb-Octβ2R) that modulates the octopamine receptor in *Drosophila*. We demonstrate that *stuxnet* positively regulates *Octβ2R* through repression of Polycomb in the ellipsoid body of the adult fly brain and that Octβ2R is one of the major receptors mediating octopamine function in sleep homeostasis. In response to octopamine, *Octβ2R* transcription is inhibited as a result of *stuxnet* downregulation. This feedback through the Stuxnet-Polycomb-Octβ2R cascade is crucial for sleep homeostasis regulation. This study demonstrates a Stuxnet-Polycomb-Octβ2R-mediated epigenetic regulatory mechanism for octopamine reception, thus providing an example of epigenetic regulation of sleep homeostasis.

Keywords Octβ2R; Polycomb; sleep homeostasis; *stuxnet*
Subject Categories Chromatin, Transcription & Genomics; Neuroscience
DOI 10.15252/embr.201947910 | Received 12 February 2019 | Revised 16 November 2020 | Accepted 20 November 2020 | Published online 7 January 2021
EMBO Reports (2021) 22: e47910

Introduction

Drosophila has been used as a model system to study mechanisms of sleep regulation. The first studies on sleep in *Drosophila* revealed that they periodically enter a quiescence state that meets a set of criteria for sleep (Hendricks *et al*, 2000; Shaw *et al*, 2000). *Drosophila* sleep is monitored normally by a *Drosophila* activity monitoring system (DAMS) and is defined as immobility for 5 min or longer which is a sleep bout. *Drosophila* sleep mainly happens at night, while a period of siesta is in the mid-day. For example, total sleep time is around 380 min (male) and 250 min (female) during the day time, and 480 min (male) and 490 min (female) during the night time in w^{1118}.

In *Drosophila*, central complex structures, especially the ellipsoid body (EB) and fan-shaped body (FSB), are important for sleep homeostasis regulation. Activation of dorsal FSB neurons is sufficient to induce sleep (Donlea *et al*, 2011). The dorsal FSB also integrates some sleep inhibiting signals (Liu *et al*, 2012). Both dorsal FSB and EB ring 2 are important in sleep homeostasis (Donlea *et al*, 2014; Liu *et al*, 2016; Pimentel *et al*, 2016). Recently, the helicon cells were found to connect the dorsal FSB and EB Ring 2 (Donlea *et al*, 2018), indicating that these EB and FSB are connected.

Multiple studies indicate that the epigenetic mechanisms are involved in circadian regulation (Etchegaray *et al*, 2003; Doi *et al*, 2006; Nakahata *et al*, 2008; Valekunja *et al*, 2012; Aguilar-Arnal & Sassone-Corsi, 2015; Tamayo *et al*, 2015; Xu *et al*, 2016). However, a direct link between epigenetic regulation and sleep homeostasis is not yet established.

Octopamine (OA) in *Drosophila* is a counterpart of vertebrate noradrenaline. Previous studies in *Drosophila* showed that OA is a wake-promoting neurotransmitter and plays an important role in regulating both sleep amount and sleep homeostasis. The mutants of the OA synthesis pathway show an increased total sleep (Crocker & Sehgal, 2008). Activation of OA signaling inhibits sleep homeostasis (Seidner *et al*, 2015), while in OA synthesis pathway mutants, an enhanced sleep homeostasis is observed (Crocker & Sehgal, 2008). Study of the neural circuit responsible for the sleep/wake effect of OA showed that octopaminergic ASM neurons (Busch *et al*, 2009) project to the pars intercerebralis (PI), where OAMB (one of the OA receptors)-expressing insulin-like peptide (ILP)-secreting neurons act as downstream mediators of OA signaling (Crocker *et al*, 2010). However, the effects of manipulating ASM neurons or ILP-secreting neurons are much weaker than those observed by manipulating all OA secreting neurons (Dubowy & Sehgal, 2017). Moreover, the effect of octopamine is not completely suppressed in the $OAMB^{286}$ mutant (Crocker *et al*, 2010), arguing that another receptor or circuit may participate in this process.

Eight OA receptors are identified to date: OAMB, Octβ1R, Octβ2R, Octβ3R, TAR1, TAR2, TAR3, and Octα2R (Qi *et al*, 2017).

1 Department of Entomology, MOA Key Lab of Pest Monitoring and Green Management, College of Plant Protection, China Agricultural University, Beijing, China
2 MOE Key Laboratory of Cell Proliferation and Differentiation, School of Life Sciences, Peking-Tsinghua Center for Life Sciences, Academy for Advanced Interdisciplinary Studies, Peking University, Beijing, China
*Corresponding author. Tel: +86 15120098776; E-mail: dujuan9981@cau.edu.cn
†These authors contributed equally to this work.

© 2021 The Authors

Although the expression pattern of OA is identified (Busch *et al*, 2009), the endogenous expression profile of these receptors is lacking (El-Kholy *et al*, 2015). A previous study demonstrated that the mushroom body-expressed OAMB mediates the sleep:wake effect of OA (Crocker *et al*, 2010). Recently, Octβ2R was shown to be important for the OA effect on endurance exercise adaptation (Sujkowski *et al*, 2017). How the versatility of OA function is mediated by the diverse array of its receptors needs further study. Moreover, the upstream regulatory mechanisms of OA receptors are still unknown.

In a previous study, we showed that Stuxnet (Stx) is important in mediating Polycomb (Pc) protein degradation in the proteasome (Du *et al*, 2016). Stx, which is an ubiquitin like protein, mediates Polycomb (Pc) protein degradation through binding to the proteasome with a UBL domain at its N terminus and to Polycomb through a Pc-binding domain. Stx level changes result in a series of homeotic transformation phenotypes. Pc is an epigenetic regulator functioning in Polycomb Group (PcG) Complexes. Although it is reported that PcG component E(Z) is involved in circadian regulation (Etchegaray *et al*, 2006), the role of *stx* in adult physiological process is unknown.

In this study, we identified the role of the epigenetic regulator Stx in sleep regulation. We found that Stx positively regulates *Octβ2R* through regulation of *Polycomb* in the EB of the adult fly brain. Further study demonstrated that the Stuxnet-Polycomb-Octβ2R cascade plays an important role in sleep regulation. In order to elucidate the role of this Stuxnet-Polycomb-Octβ2R cascade in sleep regulation, we systematically identified the role of various Octβ receptors in sleep regulation. We found that *Octβ2R* was one of the receptors that mediates OA function in sleep homeostasis. More interestingly, we found that *stx* was OA-responsive depending on the *Octβ1R*. Based on our data, we propose that the Stuxnet-Polycomb-Octβ2R cascade provides a feedback mechanism for OA signals to the EB to regulate sleep homeostasis and sleep amount.

Results

Stuxnet (stx) is involved in sleep regulation in adult *Drosophila*

In a *Drosophila* genetic screen for sleep regulators, we found that mutation of *stx* leads to increased sleep. We tested this with two different alleles—stx^{d77}, which was generated by imprecise P element excision (Du *et al*, 2016) (Fig EV1A), and stx^{34}, which was made by CRISPR-Cas9-mediated deletion of exon 3 and exon 4 in the *stx* gene region (Fig EV1B). The hemizygous males of both stx^{34} and stx^{d77} show increased total daytime sleep, caused by increases of sleep bout duration and decreases of sleep bout number (Fig 1A–D and F–I). Although the total sleep at nighttime is not significantly different compared with control, the sleep quality is significantly improved with increases of sleep bout duration and decreases of sleep bout number (Fig 1A–D and F–I). These results indicate that Stx is a negative regulator of sleep. As *stx* has a role in development, we used the $Gal80^{ts}$ system (McGuire *et al*, 2003) to dissect whether the sleep defect is due to a *stx* effect on development or on adult fly neurons. After induction of *stx* RNAi before or after eclosion, we found that knockdown of *stx* in the adult fly is sufficient to cause the sleep phenotype (Fig EV1C and D), while knockdown of *stx* only before eclosion does not (Fig EV1E and F). These results show that the *stx* function on sleep is due to its effects on adult fly neurons.

In addition, we found that the sleep latency is reduced in *stx* mutants (Fig 1E and J), indicating an increased sleep pressure in the mutants. In the sleep deprivation test, *stx* mutants still have a significant sleep recovery. Further analysis showed that both of the *stx* mutants have significant increases on the sleep recovery after sleep deprivation during the nighttime (Fig 1K–N) and during the day time (Fig EV1G–J), indicating an increased sleep pressure when *stx* function is defective. These results suggest that *stx* plays a critical role on sleep homeostasis. Both of the *stx* mutants are verified to have normal activity by the group activity profile, wake activity (Fig EV1K and L), and climbing test (Fig EV1M and N).

In order to identify the expression pattern of *stx* gene, we did antibody staining in adult fly brains. The validity of the antibody was proven by the detection of the endogenous *stx* in hh-Gal4, *stx* RNAi fly wing disk. We found that Stx staining is significantly down in the RNAi compartment (Fig EV2A–D). In addition, Stx is colocalized at least partially with DAPI staining (Fig EV2E–H). In the adult fly brain, *stx* is expressed in the central complex neurons in the EB (Fig 2A–D′) and in most of the neuronal perikarya (Fig 2A′–D′ and E′–H′). The specificity of the brain staining is verified by loss of most of the signal in *stx* mutants (Fig EV2I–K).

The expression pattern of *stx*-Gal4-driven fluorescent proteins indicates that *stx*-Gal4 (BL:62766) (Gohl *et al*, 2011) recapitulates the central complex part of *stx* expression patterns. With nuclear-localized RFP driven by *stx*-Gal4, we identified a portion of Stx-positive neurons that colocalized with RFP (Fig 2E–H′), and the position of these neurons indicates that they are colocalized in the cell body of EB neurons (Fig 2A–D′). Consistently, strong signals are detected in EB by *stx*-Gal4 driven UAS-mCD8GFP (Fig 2I). This evidence indicates that *stx*-Gal4 drives expression in a part of the EB neurons. In order to further characterize *stx*-expressing neurons, we used *stx*-Gal4 to drive expression of Denmark (Nicolaï *et al*, 2010) and Syb (Zhang *et al*, 2002) to mark axons and dendrites of these neurons, respectively. Results show that the EB and olfactory lobe are filled with axons and dendrites of these neurons (Fig 2J–L). The FB is mostly composed of axons (Fig 2M–O), while the dendrites are found outside of the EB (Fig 2J–L).

In order to validate the function of *stx* in sleep regulation, we performed overexpression of *stx* and rescue experiments. *stx* expression shows an increase in the *stx*-Gal4 line (Fig EV1O). Overexpression of *stx* driven by *stx*-Gal4 results in sleep decrease (Fig EV2L). Over regulation of *stx* driven by *EB1*-Gal4 results in sleep decrease (Fig 2Q). Overexpression of *stx* driven by both *stx*-Gal4 and EB1-Gal4 driving expression in the EB Ring 2 (R2) (Young & Armstrong, 2010) rescues the *stx* mutant phenotype (rescue percentage was 36.5% in *stx*-Gal4, 135.5% in EB1-Gal4, Fig 2P and Q). By labeling the nucleus of the EB1-Gal4-expressing neurons using the nuclear-localized UAS-Red stinger, we found that a portion of Stx-positive neurons colocalized with RFP (Fig 2A–D′). Consistently, in the colocalization experiment by crossing *stx*-lexA;; EB1-Gal4 with LexAOP-FLP; UAS > stop > GFP, we found that *stx*-LexA and EB1-Gal4 colocalized in the EB R2 (Fig 2R). This evidence demonstrates that *stx* mainly functions in the EB R2.

Stx regulates sleep through *stx*-Polycomb-*Octβ2R* cascade

Stx was previously shown as a Pc stability control factor in developmental processes of various tissues (Du *et al*, 2016). In this study,

 © 2021 The Authors

we found that Pc is also a sleep regulator. In the Pc^{XT109} mutant, total daytime sleep amount and daytime sleep duration are down-regulated, while daytime sleep number is up-regulated (Fig 3A–C). In order to determine the molecular mechanisms of *stx* function on sleep regulation, we tested whether *stx* regulation on sleep is dependent on *Pc*. Results showed that removing one copy of *Pc* could rescue the sleep phenotype of stx^{d77} hemizygous mutants (percentage of rescue for stx^{d77} was 128.6% for total day sleep, 109.6% for day sleep bout duration, 140.4% for day sleep bout number, 29.86% for sleep latency, Fig 3A–D), indicating that *Pc* is downstream of *stx* in the sleep regulation pathway. This is consistent with the previous finding that Stx stabilize Pc through proteasome-dependent pathway (Du *et al*, 2016).

In order to find out the Pc target genes responsible for sleep in *stx* mutant, we performed RNA-seq analysis in head tissues of control versus stx^{d77} adult flies (NCBI bioproject: PRJNA513466). By comparing the differentially expressed genes found in RNA-seq with the known Polycomb-binding genes in modENCODE website to look for potential Pc target genes, we finally focused on the *octopamine β2 receptor* (*Octβ2R*), which is downregulated in stx^{d77} flies, and confirmed this by quantitative RT–PCR (Fig 3E).

Further analysis demonstrated that *stx* regulates sleep through a *stx*-Polycomb-*Octβ2R* cascade. Rescue experiment showed that EB1-Gal4-driven *Octβ2R* could rescue the *stx* phenotype (percentage of rescue is 24.4%, Fig 3F). Moreover, EB1-Gal4 driven *Pc RNAi* could rescue the *stx* phenotype (percentage of rescue is 43.2%, Fig 3G). Consistent with this, *Octβ2R*-Gal4 is expressed in the central complex (Fig EV3A–F), which overlaps with *stx* expression patterns in the EB (Fig 3H). Based on these results, we propose that the *stx*-Polycomb-*Octβ2R* regulatory cascade is responsible for sleep regulation.

In order to find out if *Octβ2R* was a direct target of Polycomb in the adult fly brain, we applied tissue-specific Dam-ID (Southall *et al*, 2013; Marshall *et al*, 2016) to identify whether Pc binds on the genomic region of *Octβ2R*. We tested 12 pairs of primers spanning the *Octβ2R* locus (Fig 3I) and found that Pc has significant binding on the region near transcriptional start sites (Fig 3J). Consistent with this, the *Octβ2R* mRNA is up-regulated in Pc^{XT109} flies (Fig 3K).

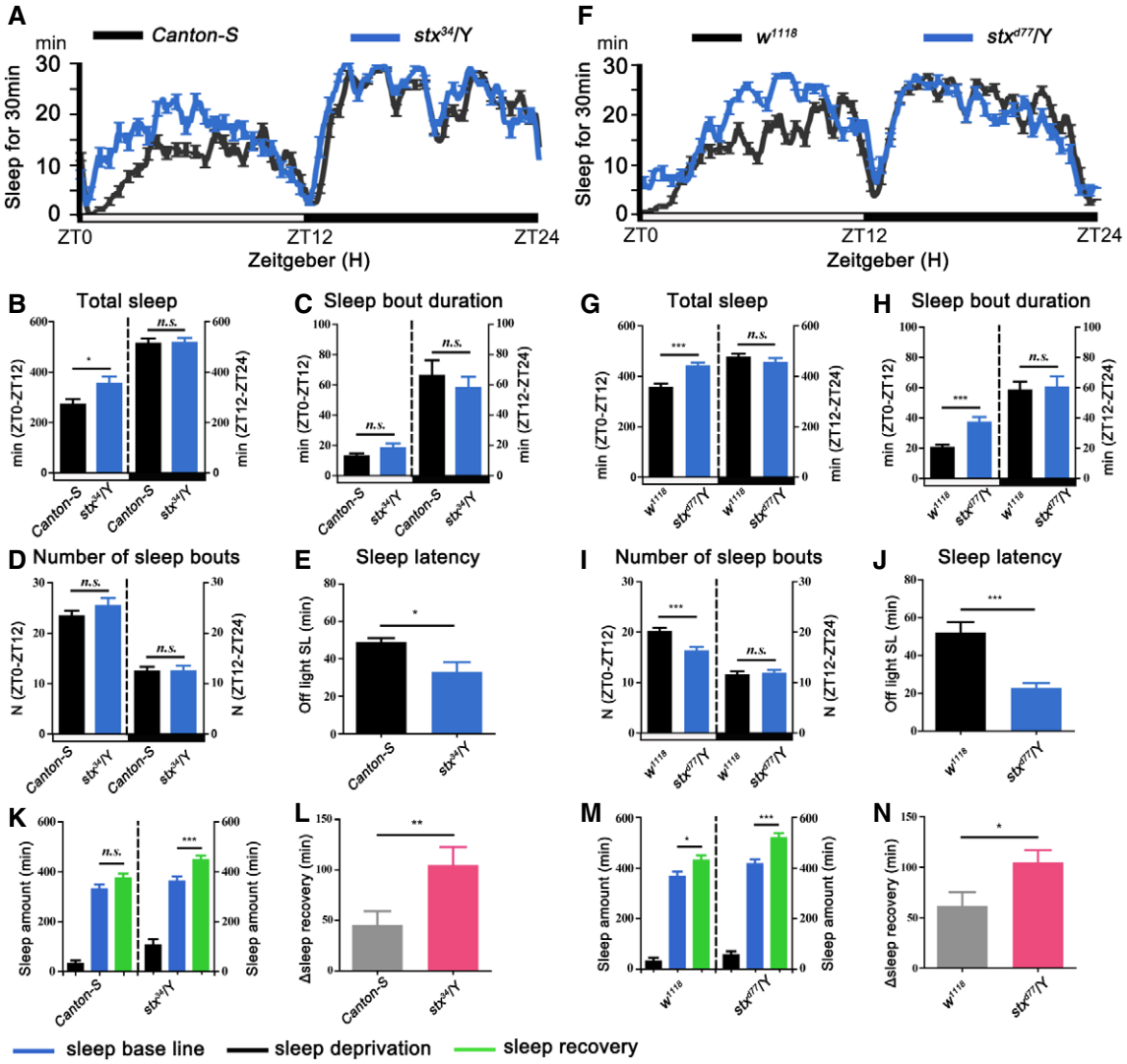

Figure 1.

Figure 1. *Stuxnet (stx)* is involved in sleep regulation in adult *Drosophila*.

A–E Statistical analysis of *stx* mutant stx^{34} sleep profile compared with that of the *Canton-S* control. (A) 24-h sleep curve (*y*-axis was average sleep time in every 30 min), $n = 16$. (B) Total sleep (From left to right mean ± SEM: 275.8 ± 17.08, $n = 47$; 358.6 ± 23.47, $n = 39$; 517.0 ± 16.49, $n = 47$; 519.7 ± 15.89, $n = 39$). (C) Sleep bout duration (From left to right mean ± SEM: 13.04 ± 1.287, $n = 47$; 18.01 ± 2.212, $n = 39$; 66.70 ± 9.569, $n = 47$; 59.41 ± 6.909, $n = 39$). (D) Number of sleep bouts (From left to right mean ± SEM: 23.61.5 ± 0.882, $n = 47$; 25.95 ± 1.353, $n = 39$; 12.64 ± 0.713, $n = 47$; 12.44 ± 0.888, $n = 39$). (E) sleep latency (From left to right mean ± SEM: 49.00 ± 2.041, $N = 4$; 33.09 ± 5.100, $N = 4$).

F–J Statistical analysis of *stx* mutant stx^{d77} sleep profile compared with control w^{1118}. (F) 24-h-sleep curve, $n = 16$. (G) Total sleep (From left to right mean ± SEM: 359.0 ± 12.91, $n = 64$; 444.5 ± 10.98, $n = 74$; 478.9 ± 10.76, $n = 64$; 458.1 ± 13.98, $n = 74$). (H) Sleep bout duration (From left to right mean ± SEM: 21.01 ± 1.312, $n = 64$; 37.63 ± 2.988, $n = 74$; 58.81 ± 5.202, $n = 64$; 61.0 ± 6.555, $n = 74$). (I) Number of sleep bouts (From left to right mean ± SEM: 20.23 ± 0.627, $n = 64$; 16.38 ± 0.693, $n = 74$; 11.66 ± 0.605, $n = 64$; 11.93 ± 0.556, $n = 74$). (J) Sleep latency (From left to right mean ± SEM: 52.20 ± 5.496, $N = 7$; 22.76 ± 2.621, $N = 9$).

K–N Sleep deprivation test of *stx* mutants. (K, L) 12-h mechanical night sleep deprivation was performed in stx^{34} and *Canton-S* control. (For K, from left to right mean ± SEM: 34.53 ± 9.85, $n = 53$; 334.2 ± 14.34, $n = 53$; 378.8 ± 14.20, $n = 53$; 108.8 ± 20.73, $n = 47$; 361.1 ± 16.71, $n = 47$; 450.8 ± 14.84, $n = 47$; for L, from left to right mean ± SEM: 45.60 ± 13.43, $n = 53$; 104.9 ± 17.70, $n = 47$). (M, N) 12-h mechanical night sleep deprivation was performed in stx^{d77} and w^{1118} control. Sleep amount calculation of deprived night sleep (Deprivation), the day sleep amount of previous day (Baseline), and the day sleep amount after the deprivation (Recovery; For M, from left to right mean ± SEM: 35.06 ± 10.76, $n = 50$; 370.8 ± 16.07, $n = 50$; 434.5 ± 17.42, $n = 50$; 59.36 ± 11.59, $n = 53$; 420.3 ± 15.60, $n = 53$; 523.9 ± 15.12, $n = 53$; For *N*, from left to right mean ± SEM: 61.86 ± 13.35, $n = 50$; 104.0 ± 11.86, $n = 53$) (K, M). Increased sleep amount in the recovery sleep comparing to the Baseline (L, N), which was calculated by the subtraction of the day sleep amount after the deprivation (Recovery) by the day sleep amount of previous day (Baseline).

Data information: Bar graphs are presented as mean ± SEM. (B–D, G–I, K, M) Statistical differences were measured using non-parametric test with two-tailed Mann–Whitney test, n.s. indicates no significant difference, $*P < 0.05$, $**P < 0.01$, $***P < 0.001$. (E, J, L, N) Statistical differences were measured using unpaired Student's *t*-test, $*P < 0.05$, $**P < 0.01$, $***P < 0.001$. *n* indicates the number of tested flies, *N* indicates the number of biological repetitions. Horizontal white and black boxes along the *x*-axis indicate light and dark periods under LD, respectively. All the *P*-values are listed in Table EV3.
Source data are available online for this figure.

These data collectively validate the regulatory cascade of *stx*-Polycomb-*Octβ2R*.

Identification of *Octβ1R*, *Octβ2R*, and *Octβ3R* roles in OA function in sleep regulation

Octopamine synthesis defects lead to sleep increase and sleep latency reduction (Crocker & Sehgal, 2008). OAMB was previous reported to mediate OA function (Crocker *et al*, 2010). Are *Octβ* receptors mediating OA function on sleep? Among all these OA receptors, is *Octβ2R* exclusively buffered by a regulatory cascade and, if so, why?

In order to answer these questions, we checked whether *Octβ2R* was the only beta receptor buffered by this regulatory cascade. Results showed that the *Octβ1R* and *Octβ3R* are not regulated by *stx* (Fig EV3G and H). No significant Polycomb binding was found on *Octβ1R* locus (Fig EV3G), although Polycomb binding was found on *Octβ3R* locus (Fig EV3H).

Next, we checked the sleep phenotypes of mutants of various *Octβ* receptors, in which the transcription of the receptors was downregulated (Fig EV3I–K). Results showed that mutations of multiple *Octβ* receptors lead to sleep increase. In the homozygous alleles of these 3 *Octβ* receptors, sleep is significantly increased (Fig 4A–C, Table EV1). Compared with the control flies, treatment of *Octβ1R, Octβ2R,* and *Octβ3R* homozygous mutants with OA results in partial rescue of the sleep decreasing phenotype (Fig 4D–F), indicating that *Octβ1R, Octβ2R,* and *Octβ3R* function redundantly in OA mediated sleep amount reduction. Furthermore, we compared the phenotypes of double and triple mutants with single heterozygous mutants. We found that both double and triple mutants show enhanced phenotypes (Fig 4G and H). So, in the regulation of sleep amount, these 3 OA receptors are redundant.

Previous results indicated that the activation of OA-producing neurons abolishes sleep homeostasis (Seidner *et al*, 2015). However, the responsible receptors were unknown. In sleep deprivation experiments, results showed that three *Octβ* receptors have different roles in mediating the OA function on sleep homeostasis. The mutation of *Octβ1R* leads to more sleep recovery after sleep deprivation, and it has same response to OA treatment as w^{1118} controls (Fig 4I), indicating that *Octβ1R* is not responsible for OA-induced loss of sleep recovery. Compared with w^{1118} controls, *Octβ2R* and *Octβ3R* mutants have more sleep recovery after sleep deprivation (Fig 4J and K). Moreover, *Octβ2R* and *Octβ3R* mutants could rescue the OA-induced downregulation of the sleep recovery phenotype (Fig 4J and K). These results indicate that the *Octβ2R* and *Octβ3R* are responsible for the OA function in sleep homeostasis.

The *Octβ2R* and *Octβ3R* play different roles in regulating sleep homeostasis. *Octβ2R* loss induced a significant higher sleep pressure in the presence of OA (Fig 4J). This phenotype is consistent with *stx* mutant phenotype (Fig 1K–N). Although *Octβ3R* mutations could partially rescue the OA-induced loss of sleep recovery, it has the similar trend of response to OA treatment comparing to w^{1118} controls (Fig 4K). This result suggests that *Octβ2R* is more sensitive to sleep pressure changes in response to OA. All three *Octβ* receptors are functional OA receptors as mutations of them showed a sleep increase phenotype (Fig 4A–C) as well as partial rescue of the sleep decrease phenotype in response to OA (Fig 4D–F). The difference of the function of these three *Octβ* receptors probably is because the three receptors have different sensitivity to OA molecules or different connection circuits of neurons expressing certain receptors.

There were discrepancies in the sleep phenotype of octopamine pathway mutants detected by video-based method versus DAM-based method. The knockout allele of *Octβ2R* receptor showed different phenotype in video-based method versus DAM-based method (Deng *et al*, 2019). In order to find out whether this is the case for mutants of *Octβ2R* receptor used in our study, we established Big Brother video tracking system in the laboratory to verify the phenotypes. Multiple alleles of *Octβ2R* show an increase in total sleep (Fig 4L). In conclusion, multiple *Octβ2R* mutants used in this study showed the same phenotype through video-based method and DAM-based method.

 © 2021 The Authors

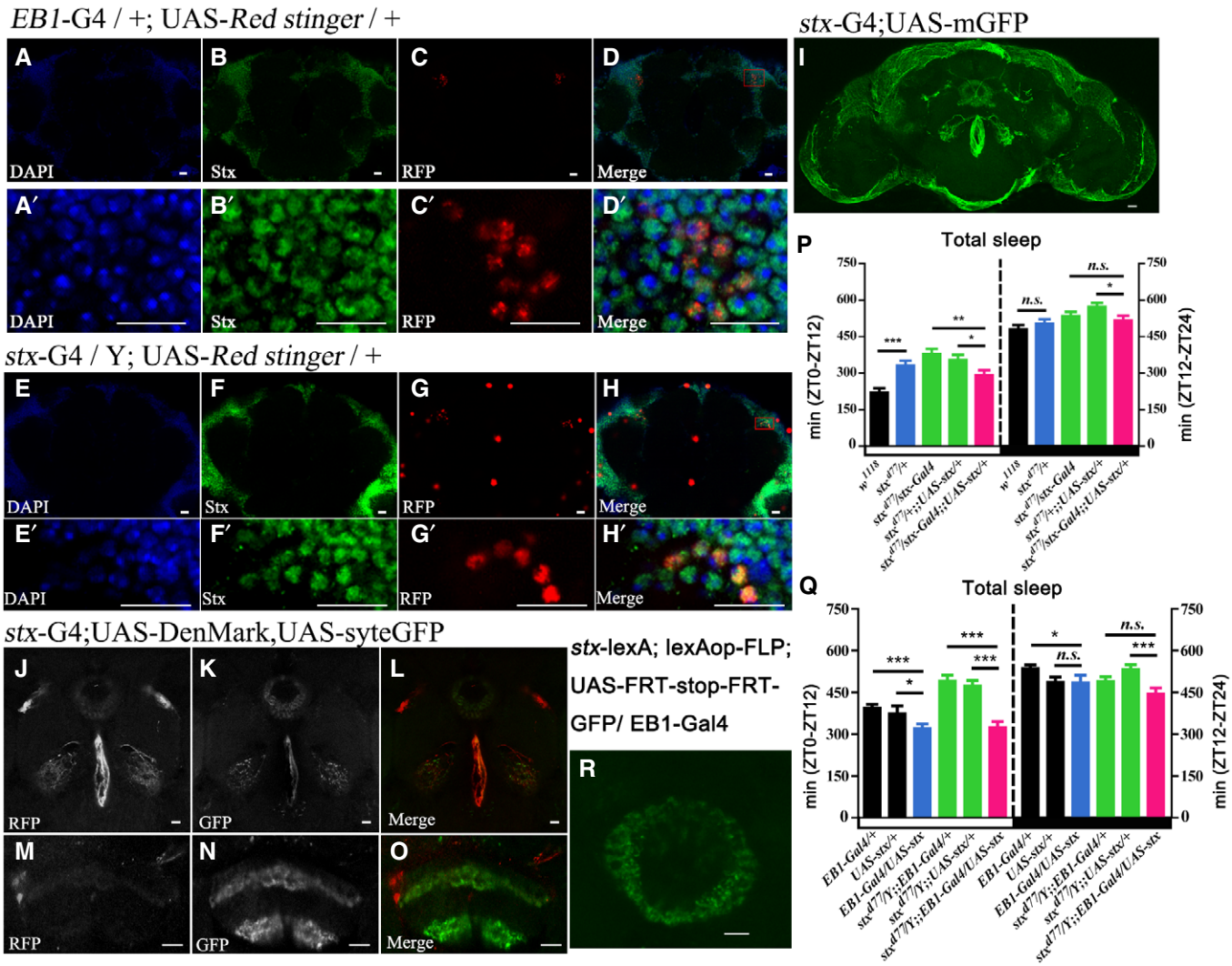

Figure 2. Characterization of *stx*-expressing neurons.

A–D′ Colocalization of Stx represented by antibody staining with EB1-Gal4. Scale bar: 10 μm.

E–H′ Colocalization of *stx* antibody staining with *stx*-Gal4 expression pattern.

I *stx*-Gal4 expression pattern shown by crossing with UAS-mCD8GFP.

J–O Dendrite (RFP) and axon (GFP) pattern of *stx*-expressing neurons. The dendrite is highlighted by Denmark (RFP), and the axons are highlighted by syt-eGFP.

P, Q Rescue experiment of *stx* mutant. The *stx* mutant phenotype can be rescued by *stx* overexpression driven by *stx*-Gal4 (in female flies, P) or EB1-Gal4 (Q). For P, from left to right females mean ± SEM: 226.0 ± 11.76, n = 49; 336.6 ± 14.10, n = 86; 382.7 ± 16.43, n = 50; 357.8 ± 16.55, n = 72; 296.2 ± 16.04, n = 68; 484.9 ± 12.97, n = 49; 507.6 ± 13.83, n = 86; 539.5 ± 12.99, n = 50. 577.0 ± 11.34, n = 72; 520.7 ± 14.96, n = 68; For Q, from left to right mean ± SEM; 398.3 ± 9.535, n = 63; 378.4 ± 23.78, n = 32; 324.4 ± 12.33, n = 45; 495.8 ± 16.43, n = 28; 478.5 ± 14.65, n = 53; 328.7 ± 16.99, n = 34; 540.7 ± 7.690, n = 63; 48 9.9 ± 21.39, n = 32; 490.9 ± 13.65, n = 45; 494.7 ± 11.99, n = 28; 537.8 ± 12.07, n = 53; 450.3 ± 15.47, n = 34.

R Colocalization of *stx*-Gal4 with EB1-Gal4. Scale bar showed was 10 μm.

Data information: Bar graphs are presented as mean ± SEM. (P, Q) Statistical differences were measured using one-way ANOVA, Tukey's multiple comparison test, n.s. indicates no significant difference, *P < 0.05, **P < 0.01, and ***P < 0.001. n indicates the number of tested flies. Horizontal white and black boxes along the x-axis indicate light and dark periods under LD, respectively.
Source data are available online for this figure.

stx-Pc-*Octβ2R* regulatory cascade modulates OA effect on sleep

In order to determine the role of this *stx*-Pc-*Octβ2R* cascade in this physiological process, we checked the function of OA on *stx*. Interestingly, we found that *stx* is feedback-regulated by OA. Tyramine β hydroxylase (TβH) is a monooxygenase and key limiting enzyme in octopamine synthesis. Both sleep amount and homeostasis were affected in a *TβH* mutant (Fig EV3L–N, also see Discussion for details). Mutated *TβH* results in a *stx* increase, while consumption of OA causes a decrease of *stx* expression level (Fig 5A and B). These results indicate that a decrease of *stx* upon the activation of OA function, suggesting that *stx* may provide a buffering mechanism

© 2021 The Authors

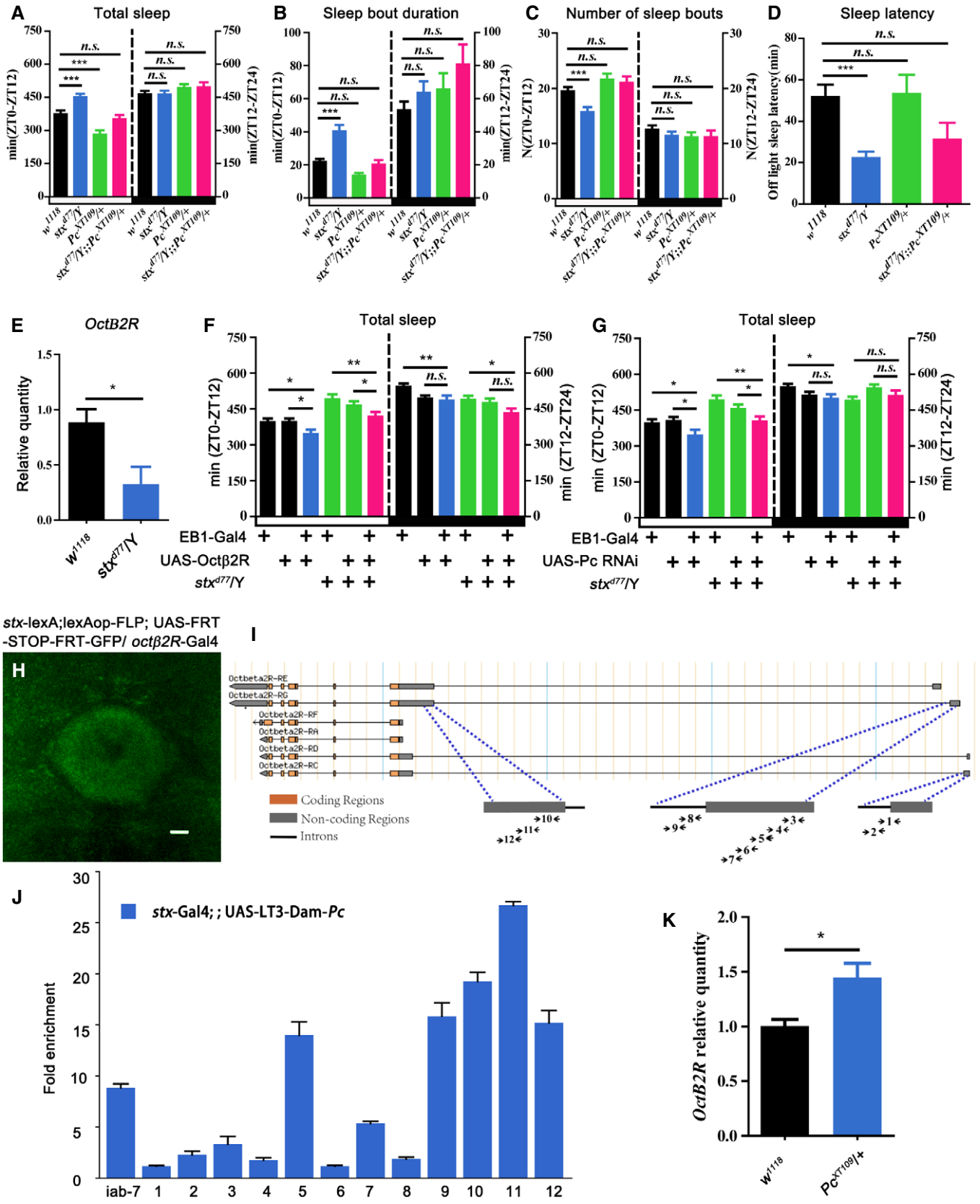

Figure 3.

© 2021 The Authors

Figure 3. Stx regulates sleep through regulating Pc downstream targets *Octβ2R*.

A–E Statistical analysis of *Pc* and *stx* double mutant stx^{d77};; pc^{XT109} sleep profile compared with controls. (A) Total sleep (From left to right mean ± SEM: 378.6 ± 12.25, n = 77; 455.0 ± 11.17, n = 80; 286.6 ± 13.68, n = 41; 356.7 ± 14.50, n = 43; 468.7 ± 10.22, n = 77; 467.2 ± 13.49, n = 80; 498.5 ± 11.91, n = 41; 500.9 ± 17.84, n = 43). (B) Sleep bout duration (From left to right mean ± SEM: 22.55 ± 1.219, n = 77; 40.86 ± 3.271, n = 80; 14.33 ± 0.889, n = 41; 20.84 ± 2.209, n = 43; 53.72 ± 4.560, n = 77; 64.26 ± 6.380, n = 80; 66.39 ± 9.010, n = 41; 81.38 ± 11.49, n = 43). (C) Number of sleep bouts (From left to right mean ± SEM: 19.67 ± 0.5610, n = 77; 15.91 ± 0.6843, n = 80; 21.79 ± 0.8670, n = 41; 21.20 ± 0.9624, n = 43; 12.69 ± 0.5957, n = 77; 11.58 ± 0.5415, n = 80; 13.31 ± 0.7201, n = 41; 11.34 ± 1.001, n = 43). (D) Sleep latency of stx^{d77};; pc^{XT109} (From left to right mean ± SEM: 52.20 ± 5.496, N = 7; 22.76 ± 2.621, N = 9; 53.68 ± 8.744, N = 3; 31.55 ± 7.770, N = 3). (E) Quantitative RT–PCR of *Octβ2R* in adult head of stx^{d77} and w^{1118} control. (Data represent mean ± SEM: w^{1118}, 0.8853 ± 0.1177; N = 3; stx^{d77}/Y, 0.3263 ± 0.1575; N = 3).

F Rescue of stx^{d77} by overexpressing *Octβ2R* in ellipsoid body. From left to right mean ± SEM: 399.6 ± 11.49, n = 50; 400.3 ± 10.48, n = 60; 349.9 ± 14.77, n = 48; 495.8 ± 16.43, n = 28; 470.1 ± 13.04, n = 44; 423.6 ± 14.32, n = 47; 548.6 ± 8.707, n = 50; 499.0 ± 8.225, n = 60; 490.7 ± 16.26, n = 48; 494.7 ± 11.99, n = 28; 480.2 ± 14.64, n = 44; 437.4 ± 14.85, n = 47.

G Rescue of stx^{d77} by *Pc RNAi* in ellipsoid body. From left to right mean ± SEM: 399.9 ± 11.88, n = 48; 409.8 ± 11.50, n = 49; 348.7 ± 20.19, n = 32; 495.8 ± 16.43, n = 28; 459.3 ± 14.78, n = 61; 407.5 ± 15.66, n = 40; 550.7 ± 8.881, n = 48; 516.0 ± 11.76, n = 49; 502.3 ± 15.08, n = 32; 494.7 ± 11.99, n = 28; 546.3 ± 11.35, n = 61; 514.2 ± 18.94, n = 40. Note that the same data is used for genotype stx^{d77};; EB1-Gal4 in panel F and G.

H Colocalization of *stx*-Gal4 with *Octβ2R*-Gal4. Scale bar showed was 10 μm.

I, J Dam-ID experiment to identify the binding of Pc on *Octβ2R* genomic locus. Primers used were shown in (I). The fold enrichment of different sites were shown in (J), *iab-7* was used as a positive control for Pc binding (From left to right mean ± SEM: 8.9 ± 0.3, 1.2 ± 0.06, 2.2 ± 0.3, 3.3 ± 0.7, 1.7 ± 0.3, 14 ± 0.06, 1.2 ± 0.3, 5.3 ± 0.7, 1.9 ± 0.3, 15.8 ± 0.06, 19.2 ± 0.3, 26.7 ± 0.7, 15.2 ± 0.7, N = 3).

K *Octβ2R* was up-regulated in Pc^{XT109} mutant (Data represent mean ± SEM: w^{1118}, 1.004 ± 0.0609, N = 3; pc^{XT109}/+, 1.447 ± 0.1300, N = 3).

Data information: Bar graphs are presented as mean ± SEM. (A–D, F, G) Statistical differences were measured using one-way ANOVA, Tukey's multiple comparison test, n.s. indicates no significant difference, *P < 0.05, **P < 0.01, and ***P < 0.001. Horizontal white and black boxes along the x-axis indicate light and dark periods under LD, respectively. (E, K) Statistical differences were measured using unpaired Student's t-test, *P < 0.05. n indicates the number of tested flies; N indicates the number of biological repetitions (For E and K, each repeat with a sample size of 30 individual fly heads; for J, each repeat with a sample size of 50 individual fly heads). All the P-values are listed in Table EV3.

Source data are available online for this figure.

to counteract OA function. The *stx* expression is up-regulated in *Octβ1R* mutant, but not in *Octβ2R* and *Octβ3R* mutants, indicating that the stx level is dependent on *Octβ1R*. Consistently, the OA effect on *stx* is not disrupted by *Octβ2R* mutation and is counteracted by *Octβ1R* and *Octβ3R* mutations (Fig 5B). These results collectively indicate that *stx* responds to OA through *Octβ1R* to tune down the production of *Octβ2R*.

Furthermore, we checked the transcription level of *Octβ2R* after feeding with OA. Results showed that *Octβ2R* transcription is down-regulated after feeding with OA (Fig 5C), and this effect was rescued by the *stx* mutation (Fig 5C).

Based on this evidence, we propose that the *stx*-Pc-*Octβ2R* regulatory cascade provides a mechanism to modulate the OA effect on sleep in the EB of the adult fly brain. Secretion of OA leads to activation of Octβ receptors as well as downregulation of *stx*. Downregulated *stx* causes a decrease of *Octβ2R* mRNA, and this prevents the overactivation of OA-Octβ2R signaling on sleep regulation. The relationship between *stx*, *Octβ1R, Octβ2R*, Pc, and OA is summarized in a simplified chart (Fig 5D).

Evidence indicates that this regulatory cascade functions in the EB. EB-specific knockdown of *Octβ2R* causes no significant change of *stx*, as is the case in the *Octβ2R* mutants of Fig 5B (Fig 5E). Meanwhile, knocking down of *Octβ2R* in the EB led to increases of sleep rebound (Fig 5F). The wake activity of EB1-Gal4-driven *Octβ2R* RNAi is comparable with controls (Fig EV3O). In response to OA, knockdown of *Octβ2R* in the EB is sufficient to rescue the sleep rebound decrease phenotype (Fig 5F).

Disruption of this regulatory mechanism results in dramatic change of sleep in the presence of OA. The sleep loss increases significantly in the Polycomb mutant after treatment with OA compared with controls. The total sleep amount decreases 13.90% on average in w^{1118} flies treated with OA, while the total sleep amount decreases 21.25% on average in Pc^{XT109} flies treated with OA (Fig 5G and H). This data demonstrate that the *stx*-Pc-*Octβ2R* cascade is an important buffering pathway compensating for the sleep decreasing effects caused by OA.

In conclusion, we identified a mechanism regulating the OA function on sleep. We found that *stx* stabilizes the OA receptor Octβ2R in EB R2 through a *stx*-Pc-*Octβ2R* regulatory cascade. *Octβ2R* mediates the OA function in both sleep and homeostasis. In the presence of OA, *stx* expression is reduced. As a result, the *Octβ2R* is downregulated to prevent the further augmentation of the OA-induced sleep and homeostasis loss effect.

Discussions

This study highlights the importance of epigenetic regulation on sleep. Although epigenetic regulation was intensively studied in adult pathological processes such as cancer, epigenetic factors have been far less studied in other physiological processes such as sleep. Our study provides an example of the maintenance role of PcG complex in sleep regulation. Although the core PcG complex component Pc is ubiquitously expressed, its regulator *stx* is tissue specifically distributed, and this distribution may keep appropriate activity of Pc as well as the PcG complex in a tissue-specific manner. The factors regulating the tissue specificity of *stx* expression need to be further investigated.

Previous study found that mutation of *Octβ2R* does not have an obvious sleep phenotype (Crocker *et al*, 2010). We carefully compared our data with the published $Octβ2R^{f05679}$ mutant data. Although $Octβ2R^{f05679}$ mutant was shown not significantly affected total sleep, we found that the $Octβ2R^{f05679}$ has mild effect on sleep, especially for males which is also found in Crocker *et al* (2010) (970.84 ± 20.89 in $Octβ2R^{f05679}$ compared with 952.59 ± 17.60 in controls). We tested other *Octβ2R* mutants and found that the male flies from these mutations indeed have sleep phenotype (Fig EV3J; Table EV1).

© 2021 The Authors

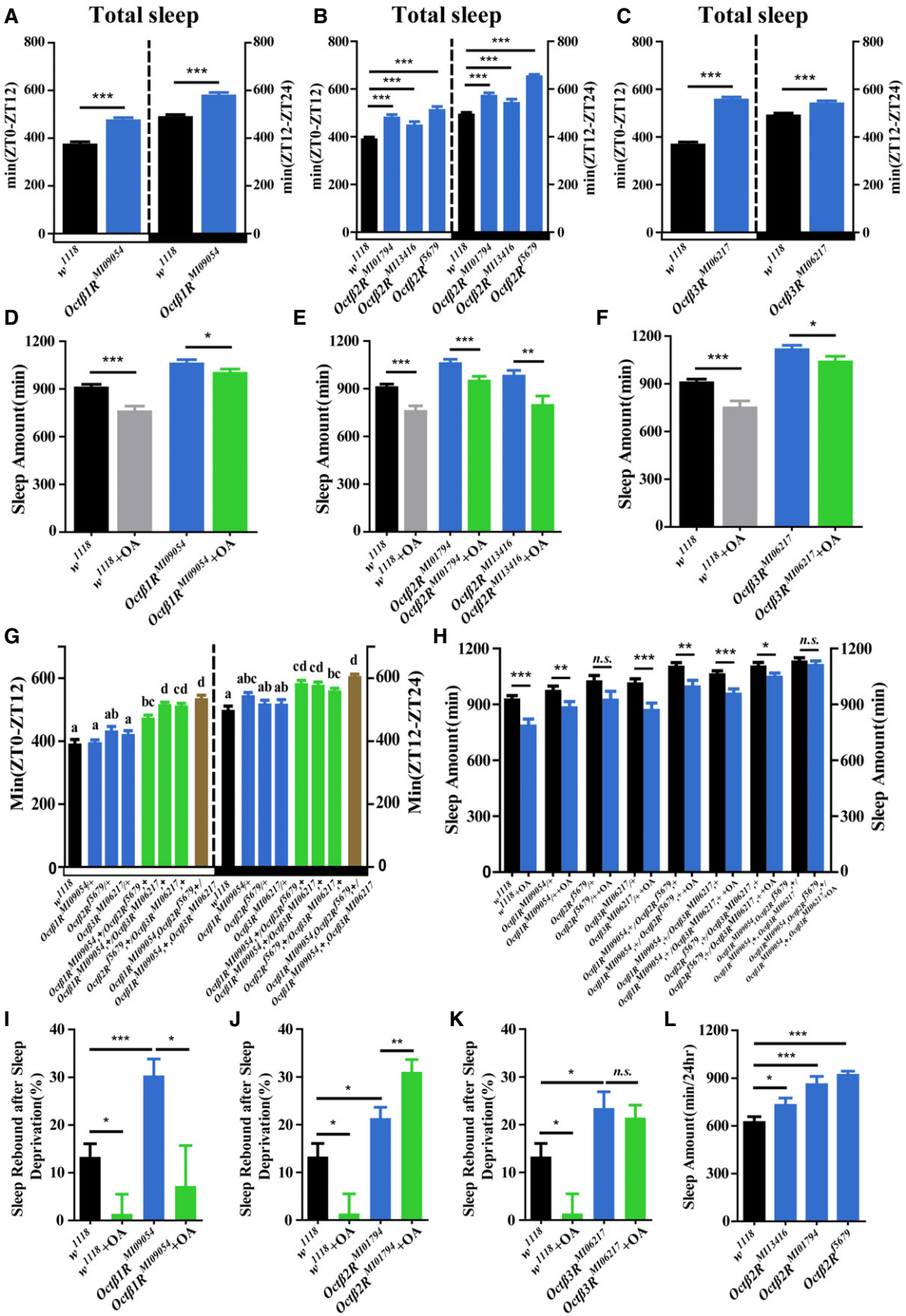

Figure 4.

© 2021 The Authors

Figure 4. Effects of different *Octβ* receptors on sleep and homeostasis.

A–C Sleep phenotype of *OctβR* mutants. Total sleep was shown in (A–C). For (A), from left to right mean ± SEM: 377.8 ± 7.389, n = 95; 479.3 ± 7.039, n = 134; 492.6 ± 6.590, n = 95; 582.8 ± 8.937; n = 134; For (B), from left to right mean ± SEM: 392.7 ± 6.385, n = 126; 484.2 ± 8.537, n = 121; 452.0 ± 11.69, n = 77; 516.4 ± 10.58; n = 55; 496.7 ± 5.618, n = 126; 575.6 ± 8.820, n = 121; 546.1 ± 11.37, n = 77; 657.9 ± 3.756, n = 55; For (C), from left to right mean ± SEM: 372.3 ± 6.483, n = 120; 560.8 ± 6.881, n = 123; 494.4 ± 5.862, n = 120; 544.8 ± 7.190; n = 123.

D–F The sleep amount after OA treatment in *OctβR* mutants comparing with w^{1118} control. (D)The sleep amount after OA treatment in *Octβ1R* mutants (From left to right mean ± SEM: 916.0 ± 13.51, n = 74; 765.1 ± 27.27, n = 60; 1,067 ± 18.23, n = 70; 1,007 ± 18.61; n = 71). (E) The sleep amount after OA treatment in *Octβ2R* mutants (From left to right mean ± SEM: 916.0 ± 13.51, n = 74; 765.1 ± 27.27, n = 60; 1,066 ± 19.12, n = 70; 956.2 ± 22.36; n = 60; 987.7 ± 27.66, n = 32; 803.3 ± 51.34, n = 23). (F) The sleep amount after OA treatment in *Octβ3R* mutants (From left to right mean ± SEM: 916.0 ± 13.51, n = 74; 765.1 ± 27.27, n = 60; 1,124 ± 18.18, n = 72; 1,047 ± 27.28; n = 58).

G Sleep phenotype of *OctβR* double and triple mutants. (From left to right mean ± SEM: 392.0 ± 12.91, n = 60; 395.1 ± 8.56, n = 79; 433.7 ± 13.03, n = 58; 422.8 ± 10.34; n = 62; 474.4 ± 8.36, n = 73; 517.4 ± 6.30, n = 119; 513.2 ± 7.10, n = 79; 536.6 ± 9.05 n = 78; 499.1 ± 11.95, n = 60; 546.0 ± 8.51, n = 79; 519.6 ± 10.31, n = 58; 518.9 ± 13.13; n = 62; 584.3 ± 8.59, n = 73; 579.2 ± 8.35, n = 119; 560.9 ± 6.80, n = 79; 606.4 ± 6.38, n = 78).

H The sleep amount after OA treatment in *OctβR* double and triple mutants comparing with w^{1118} control. (From left to right mean ± SEM: 932.6 ± 15.23, n = 38; 792.2 ± 28.87, n = 40; 978.6 ± 19.51, n = 48; 890.5 ± 25.17; n = 38; 1,030 ± 25.66, n = 36; 931.6 ± 38.73, n = 32; 1,019 ± 18.33, n = 35; 876.2 ± 31.15, n = 38; 1,1 09 ± 16.16, n = 32; 1,003 ± 26.65, n = 44; 1,067 ± 13.31, n = 44; 963.6 ± 19.95; n = 57; 1,110 ± 16.15, n = 36; 1,055 ± 13.47, n = 24; 1,136 ± 14.21, n = 64; 1,117 ± 16.77, n = 46).

I–K OA treated *OctβR* mutants and control flies have different percentage of sleep recovery after sleep deprivation. (For I, from left to right mean ± SEM: 13.31 ± 2.760, n = 51; 1.394 ± 4.107, n = 25; 30.35 ± 3.473, n = 44; 7.198 ± 8.511; n = 53. For J, from left to right mean ± SEM: 13.31 ± 2.760, n = 51; 1.394 ± 4.107, n = 25; 21.37 ± 2.244, n = 54; 31.06 ± 2.545; n = 55. For K, from left to right mean ± SEM: 13.31 ± 2.760, n = 51; 1.394 ± 4.107, n = 25; 23.48 ± 3.409, n = 70; 21.46 ± 2.629; n = 67).

L Sleep phenotype of *Octβ2R* mutants by the Video-Based Method. (From left to right mean ± SEM: 630.5 ± 27.96, n = 52; 738.0 ± 36.62, n = 20; 867.6 ± 42.99, n = 24; 926.5 ± 17.25, n = 52).

Data information: Bar graphs are presented as mean ± SEM. (A–F, H, L) Statistical differences were measured using non-parametric test with two-tailed Mann–Whitney test, n.s. indicates no significant difference, *P < 0.05, **P < 0.01, and ***P < 0.001. (G) Statistical differences were measured using one-way ANOVA, Tukey's multiple comparison test, groups with the same letter are not significantly different from each other (P > 0.05). (I–K) Statistical differences were measured using unpaired Student's t-test, n.s. indicates no significant difference, *P < 0.05, **P < 0.01, and ***P < 0.001. n indicates the number of tested flies. Horizontal white and black boxes along the x-axis indicate light and dark periods under LD, respectively. All the P-values are listed in Table EV3.
Source data are available online for this figure.

Published studies have shown that the sleep phenotype of octopamine pathway mutants is different between video-based method and DAM-based method. For example, based on DAM data, the *TβH* mutant resulted in increased sleep per day, while the same mutant showed decreased sleep based on video data (Deng *et al*, 2019). We used the video-based method to repeat the *TβH* mutant phenotype. The results showed that compared with the control flies, the *TβH* mutant got significantly less sleep (Fig 6A and B). This result is consistent with the previously published data (Deng *et al*, 2019). Through close observation of *TβH* mutant and control flies, we found that this mutant has much more frequent grooming behavior than the controls. We video recorded the *TβH* mutant and control flies for 10 min between ZT3.5 and ZT4.5. The results showed a statistically significant increase of the total number of grooming case (Fig 6C, Movies EV1–EV3). The difference between video-based method and DAM-based method is that these grooming behaviors can be detected in video-based methods, but not in DAM-based methods. Multiple studies have established a positive correlation between octopamine treatment and grooming behavior (Yellman *et al*, 1997; Weisel-Eichler *et al*, 1999; Fussnecker *et al*, 2006). Theoretically, *TβH* allele should result in a decrease in octopamine synthesis. The opposite phenotype may be caused by increased tyramine in *TβH* mutant (Crocker & Sehgal, 2008) or by other feedback regulation. The alleles for *Octβ2R* receptor used in this study show a similar grooming behavior as the control flies (Fig 6C). The previously published *octβ2R* knockout allele (Deng *et al*, 2019) should be a stronger one. The difference of sleep phenotypes between video-based and DAM-based methods may be due to the grooming behavior induced by the massive decrease of octopamine detection. Or other unrelated effects caused by the compensation effect previously reported (Teng *et al*, 2013; Rossi *et al*, 2015; Vu *et al*, 2015; Ma *et al*, 2019; El-Brolosy *et al*, 2019). One hypothesis is that the significant change of grooming behavior probably masks the sleep behavior. The relationship between grooming and sleep needs to be further clarified. The detection of the sleep phenotype without significant changes in grooming phenotype may be a better strategy to get reliable sleep phenotype. If the increase of grooming in *TβH* mutant is a side effect caused by the increased tyramine, the identification of the phenotypes of octopamine treatment or collective phenotype of octopamine receptors may be more reliable ways to draw conclusions on the function of octopamine. Furthermore, whether grooming is epistatic to sleep is a problem worthy of further study.

Two aspects of sleep homeostasis need to be further studied. First, we found that Octβ2R and stx colocalize in a subset of EB neurons. In a previously study (Liu *et al*, 2016), EB R2 neurons were found to be responsible for sleep homeostasis regulation. The relationship of these two groups of EB neurons needs further study. Second, the OA-treated *Octβ2R* mutant has more sleep recovery than the control. This indicates that OA induces more sleep recovery in the condition of *Octβ2R* downregulation. It seems that in this condition OA induces certain pathways to counteract its role in sleep homeostasis. One possibility is that *Octβ2R* negatively regulates *Octβ3R* which results in increased sleep pressure in the absence of *Octβ2R*. Further studies are needed to clarify the mechanism.

Our results suggest the *stx*-Pc-*Octβ2R* regulatory cascade serves as a buffering step for OA function in sleep homeostasis. Two-way regulation of OA on *stx* leads to reverse changes of *stx*—the more OA, the less *stx* and vice versa. Through the function of *stx*-Pc-*Octβ2R* regulatory cascade, the *Octβ2R* transcription is changed accordingly. Variation of *Octβ2R* transcription could buffer the OA response. As a result, the unfavorable effect of OA causing dramatic decrease of sleep amount and homeostasis could be compensated by its receptor.

© 2021 The Authors

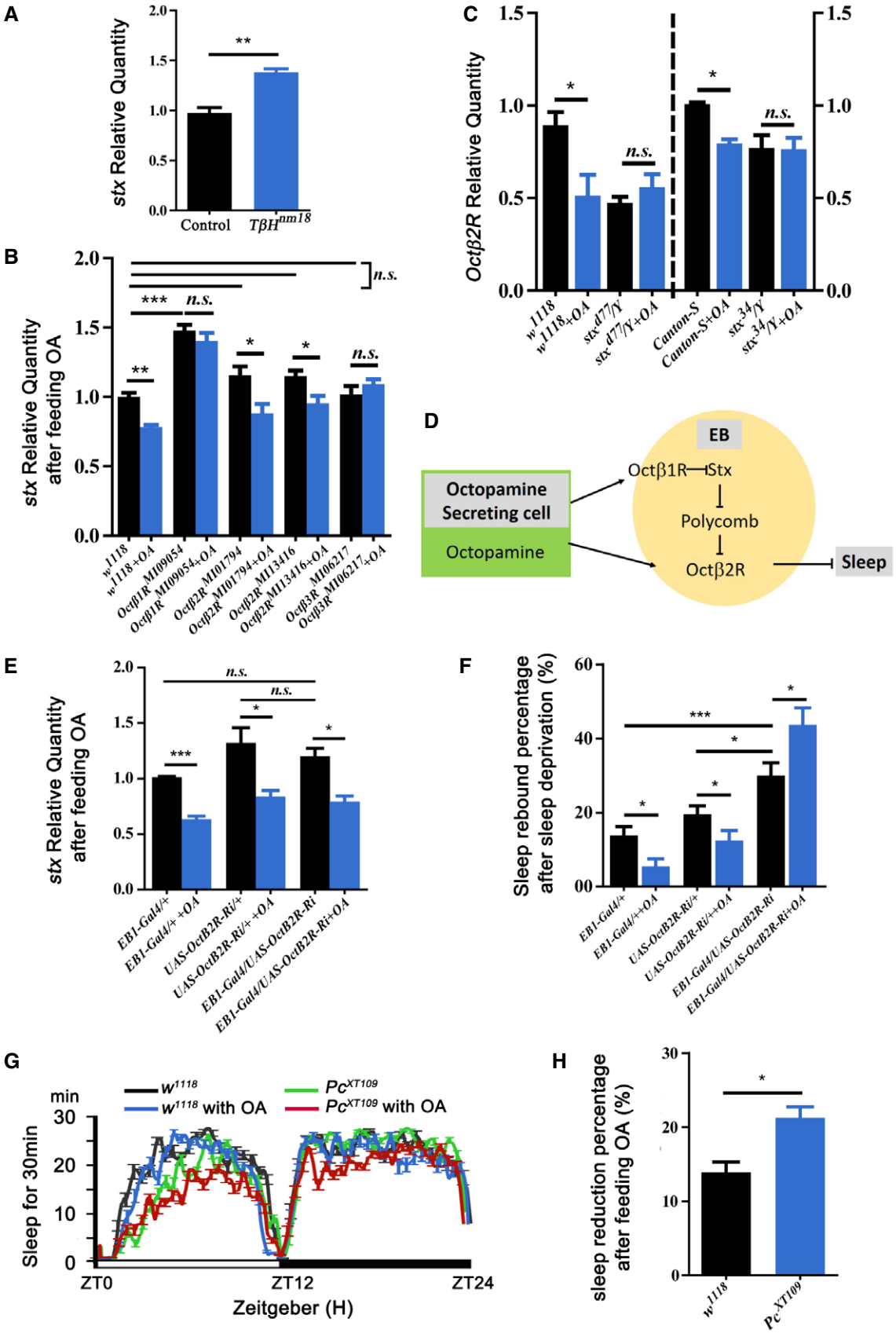

Figure 5.

© 2021 The Authors

Figure 5. *Stx* provides a buffering mechanism for *Octβ2R* expression in the presence of OA.

A Quantitative RT–PCR of *stx* in control and in mutant of the *Tβh* gene in the OA synthesis pathway. (mean ± SEM: control for *Tβh*, 0.977 ± 0.05125, $N = 3$; $Tβh^{nm18}$, 1.383 ± 0.0325, $N = 3$).

B Quantitative RT–PCR of *stx* after OA treatment in w^{1118} control and *Octβ1R*, *Octβ2R* mutants, *Octβ3R* mutants. (From left to right mean ± SEM: 1.000 ± 0.0288, 0.781 ± 0.0176, 1.477 ± 0.043, 1.403 ± 0.0578, 1.157 ± 0.0617, 0.881 ± 0.0689, 1.149 ± 0.0398, 0.953 ± 0.0543, 1.017 ± 0.0600, 1.090 ± 0.0378, $N = 3$).

C Quantitative RT–PCR of *Octβ2R* after OA treatment in wild-type control and *stx* mutants. (From left to right: mean ± SEM: 0.897 ± 0.0721, $N = 4$; 0.512 ± 0.1132, $N = 3$; 0.475 ± 0.0320, $N = 4$; 0.557 ± 0.0712, $N = 3$; 1.01 ± 0.0085, $N = 2$; 0.795 ± 0.0225, $N = 2$; 0.770 ± 0.0705, $N = 2$; 0.763 ± 0.0630, $N = 2$).

D Model of *stx* function.

E Ellipsoid body knockdown of *Octβ2R* results in no significant change of *stx*. Data represent mean ± SEM: 1.012 ± 0.006, 0.635 ± 0.027, 1.323 ± 0.136; 0.839 ± 0.055, 1.201 ± 0.072, 0.790 ± 0.052. $N = 3$.

F Ellipsoid body knockdown of *Octβ2R* results in sleep rebound increase. In response to OA, ellipsoid knockdown of *Octβ2R* rescues control phenotype. Data represent mean ± SEM: 13.80 ± 2.439, $n = 31$; 5.465 ± 2.036, $n = 25$; 19.55 ± 2.275, $n = 27$; 12.47 ± 2.684, $n = 24$; 30.03 ± 3.428, $n = 25$; 43.67 ± 4.616, $n = 25$.

G, H Sleep profile of Pc^{XT109} mutant with or without OA treatment. In both control and Pc^{XT109} mutant flies, the treatment of OA results in sleep decrease, $n = 16$ (G). Quantifications of the decreasing amount showed that Pc^{XT109} mutant fly loss significantly more sleep that control flies (From left to right mean ± SEM: 13.90 ± 1.397; 21.25 ± 1.493, $N = 4$) (H).

Data information: Bar graphs are presented as mean ± SEM. Statistical differences were measured using unpaired Student's *t*-test, and n.s. indicates no significant difference, $*P < 0.05$, $**P < 0.01$, and $***P < 0.001$. *n* indicates the number of tested flies; *N* indicates the number of biological repetitions (For A–C and E, each repeat with a sample size of 30 individual fly heads). All the *P*-values are listed in Table EV3.
Source data are available online for this figure.

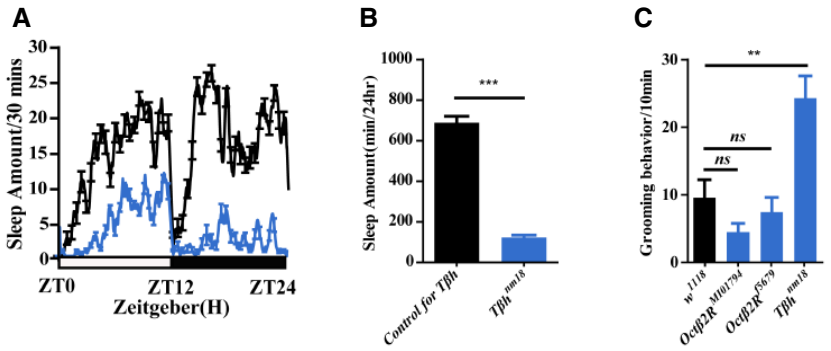

Figure 6. Phenotype identification of TβH mutant by video-based methods.

A Sleep curve for Tβh mutant and control flies in video-based method.

B Total sleep for Tβh mutant and control flies in video-based method (From left to right mean ± SEM: 688.2 ± 32.71, $n = 48$; 123.2 ± 11.68, $n = 46$).

C Number of Grooming behaviors in 10 min during ZT3.5–4.5 (From left to right mean ± SEM: 9.571 ± 2.644, $N = 7$; 4.429 ± 1.343, $N = 7$; 7.429 ± 2.170, $N = 7$; 24.29 ± 3.300, $N = 7$).

Data information: Bar graphs are presented as mean ± SEM. (B) Statistical differences were measured using non-parametric test with two-tailed Mann–Whitney test, $***P < 0.001$. (C) Statistical differences were measured using unpaired Student's *t*-test, n.s. indicates no significant difference, $**P < 0.01$. *n* indicates the number of tested flies; *N* indicates the number of biological repetitions. All the *P*-values are listed in Table EV3.
Source data are available online for this figure.

Materials and Methods

Fly stocks

The stx^{d77} mutant was generated by P hop (Du *et al*, 2016). The stx^{34} mutant was generated by deleting exon 3 and exon 4 genomic region (deletion on X: 10714349–10718262). Pc^{XT109} was a gift from Müller *et al* (1995). w^{1118} (No. 5905), UAS-DenMark, UAS-*syt*.eGFP (No. 33064), 10XUAS-mCD8GFP (No. 32184), UAS-RedStinger (No. 8547), UAS-*pc* RNAi (No. 33622), *stx*-Gal4 (No. 62766), *Octβ2R*-Gal4 (No. 67511), EB1-Gal4 (No. 44409), *Octβ2R* mutants (No. 18896, 37566, 59133), *Octβ1R* mutants (No. 51252), and *Octβ3R* mutants (No. 43050) were from the Bloomington stock center. *Octβ2R* RNAi (GD104524) and *stx* RNAi (GD27036) were from the VDRC stock center. $Tβh^{nm18}$ (*tyramine hydroxylase mutant*), *Canton-S* background control (control for $Tβh^{nm18}$), UAS-Oct*β2R*, LexAOP-FLP; UAS > stop > GFP, and *Canton-S* flies were from Yi Rao's laboratory (Peking University, China). UAS-*stx* was generated in a previous study (Du *et al*, 2016). *stx*-lexA was generated based on *stx*-Gal4 by using the InSITE system (Gohl *et al*, 2011).

CRIPSPR-Cas9 generation of the stx^{34} mutant

For CG32676 knockout, two sgRNAs were designed to target the upstream of exon3 and downstream of stop codon, respectively, which can bring about 4kb deletion to the gene. The sgRNAs' sequences are KO-5sg1: GGGGGGATGGGGCGGTGCAGGG and KO-5sg2: GATAAAGTCAGCGGGGCTGGTGG. 15 μg of Cas9 mRNA and 7.5 μg sgRNA were mixed with DEPC water in a 30 μl volume. And the RNA mix injection was performed by Fungene Biotech (http://www.fungene.tech) for injection and screening transgenic flies. Embryos were injected using standard protocols. Injections were

© 2021 The Authors

carried out at 18°C, and embryos were shifted to 25°C immediately following injection. When the P0 and F1 flies grew into adults, they were crossed with *FM7a*. The genomic DNA of the P0 and F1 flies was extracted. PCR was performed using primers flanking the knockout region. Amplified products were purified for Sanger sequencing to validate the deletion. Primers used for verification are 32676 KO-F: CATCCACAGTTCAGTTCATT; 32676 KO-R: GCTGGTT CATTCACTTCATTTGC.

Drosophila Activity Monitor-based method for activity measurement, sleep deprivation, and sleep analysis

For all activity measurements unless specified, all flies were kept on a 12-h light/12-h dark cycle (3,600 lux of light) at 25°C Flies (4–7 days old) were loaded individually into detecting tubes (length, 65 mm; inner diameter, 5 mm) containing standard cornmeal fly food unless specified at one end, and a cotton stopper was placed on the other end. Sleep behavior was measured using a DAM (Trikinetics, MA, U.S.), which counts the infrared beam crossing of individual flies in each tube every 1 min. Flies were entrained in detecting tubes for 24–36 h at 25°C in an LD cycle, and then, data were collected in LD for at least 3 days with the DAM System. Analyses of total sleep, sleep bout duration, and number of sleep bouts were carried out using with Pysolo software (obtained from the website http://www.pysolo.net). Sleep latency was defined as a period of time from the moment lights are turned off to the first bout of sleep (Crocker *et al*, 2010). Sleep latency was analyzed with Pysolo software (obtained from the websites: http://www.pysolo.net) and MATLAB (MathWorks, Natick, MA).

Mechanical sleep deprivation was performed using the SNAP method to keep flies awake for 12 h overnight (Shaw *et al*, 2002). Flies were sleep deprived from ZT12 (beginning of the dark phase) to ZT0 (beginning of the light phase) by vortexing at the lower intensity setting for vortexing for 3 s every minute. All sleep deprivation is at night except for experiments shown in Fig EV1G–J in which flies were day time sleep deprived using the same setting from ZT0 (beginning of the light phase) to ZT12 (beginning of the dark phase). Sleep lost and recovery were calculated for each fly by using the 24-h period preceding deprivation as the baseline. Sleep recovery values were calculated by sleep amount after deprivation minus sleep amount of the corresponding time of the previous day (baseline sleep amount). Sleep rebound percentage was calculated by the following formula: (sleep amount after deprivation − baseline sleep amount)/lost sleep amount during deprivation.

Percentages of rescue were calculated by (rescued-mutant)/(control-mutant).

All statistical tests were performed by prism5.0 (GraphPad Software). The statistical tests for each experiment are shown in the figures. All the *P*-values are listed in Table EV3. Bar graphs are presented as mean ± SEM. two-tailed Mann–Whitney test was used to compare two samples. One-way ANOVA followed by Tukey *post hoc* test (Prism GraphPad) was used for multiple comparisons. *n*.s. indicates no significant difference, * indicates $P < 0.05$, ** indicates $P < 0.01$, and *** indicates $P < 0.001$.

All behavior tests were performed in isogenous backgrounds. Female stx^{d77} flies were out crossed to w^{1118} for seven generations to clean up the genetic background. The stx^{34} was made from *Canton-S* flies. The specific line for generating the mutants was used as controls for sleep analysis. The *Canton-S* background control is used for $T\beta H^{nm18}$ mutant. The *stx*-Gal4 and *stx*-lexA are generated in w^{1118} background. All *octβR* mutants were outcrossed seven generations with w^{1118} (No. 5905). All genotypes are verified using PCR.

All behavior tests were done with at least 3 repeats, each repeat with a sample size of 16 individual flies. The sample size was determined in Rosato & Kyriacou (2006). Flies of certain genotypes used for tests were randomly selected. Steps for blinding of the investigators were taken to minimize the subjective bias when analyzing the data. All sleep tests were done in males except when annotated.

Video tracking method for sleep analysis

Sleep analysis was performed using a video-based recording system (Big Brother video system from Big Brother, Coulbourn Instruments, Wilmette, IL) which can be adapted for activity tracking for mouse and insects (Vitaterna *et al*, 2006; Ludin *et al*, 2016). Flies aged 3–5 days were placed in 24-well plates containing fly food (2% Agar and 5% Sucrose). Before sleep recording, flies were entrained for 24–36 h in a 12 h light: 12 h dark cycle at 25°C. Sleep behavior was recorded by video cameras with 628 × 582 resolution. In order to provide constant illumination in the dark period, we used infrared LED lights. Videos were taken at four frames per second (In other words, Big Brother locates each fly four times per second). The program (Big Brother video system) measures the distance travelled by the animal between each frame. Camera noise will sometimes make the calculated location bounce around by a few pixels, even if the animal does not move. The threshold setting is designed to screen out this random or unwanted signal. The program will detect and measure motion from frame to frame if the animal moves more than the number of pixels indicated by motion(activity) threshold setting. We set different motion thresholds (e.g. threshold = 1, 2, 3, 4) to test camera noise by recording from dead flies. When the motion threshold is set to 4, the signals from dead flies can be ignored. This setting is used in this study. The resulting data were analyzed and viewed by the Big Brother analysis component. We used the Big Brother File utility to separate the data from each cell into Pysolo compatible file. The data were analyzed for sleep parameters with Pysolo software (obtained from the website http://www.pysolo.net). Sleep was defined with more than 5 min bout of inactivity (Shaw *et al*, 2000).

OA treatment assays

Octopamine powder (Sigma, #O0250) was dissolved in water to prepare a stock solution for feeding OA experiments. This stock solution was diluted in standard cornmeal fly food to prepare 5 mg/ml of OA-containing food.

For the feeding OA and behavior assay, the newly eclosed flies were placed in standard fly food for 4–7 days, and then, the flies were loaded either to detecting tubes containing standard fly food plus 5 mg/ml OA or onto standard fly food alone. As described above, flies were entrained in detecting tubes for 24–36 h at 25°C in an LD cycle, and then, data were collected in LD for at least 3 days with the DAM System in 1 min bins.

All OA treatment assays were done with at least 3 repeats, each repeat with a sample size of 16 individual flies.

 © 2021 The Authors

Immunofluorescence experiments

Adult flies that were 7–15 days old (unless otherwise noted) were anaesthetized with CO_2 and dissected in 0.03% PBST (1 × PBS with 0.03% Triton X-100; Sigma, T9284) on ice. After a 55 min fixation of samples in 2% paraformaldehyde (PFA) at room temperature (RT), samples were washed four times for 15 min in 0.03% PBST at RT, blocked in 10% Normal Goat Serum (NGS; diluted with 1 × PBS with 2% Triton) overnight at 4°C and incubated with primary antibodies for two overnights at 4°C. The samples were washed again four times with 1 × PBS with 1% Triton for 15 min at RT and incubated with secondary antibodies for two overnights at 4°C. And then the samples were washed with 1 × PBS with 1% Triton again 4 times for 15 min at RT and mounted on a slide using anti-fading Mounting medium (with DAPI; Solarbio, S2110). The primary and secondary antibodies were diluted in dilution buffer (1.25% PBST, 1% NGS). The primary antibodies used in this study were anti-GFP rabbit (Thermo Fisher Scientific, #A11122; 1:500) and anti-Stx rabbit (Gift from Alan Zhu's laboratory, 1:500). The secondary antibodies were diluted at 1:200 and were as follows: goat anti-rabbit Alexa Fluor 564 and goat anti-mouse Alexa Fluor 488. Images were taken using confocal microscopy (Leica SP8) with LAX software with auto Z brightness correction to generate a homogeneous signal where it seemed necessary and were formatted using Adobe Photoshop CS6. Figures were generated using Adobe Photoshop CS6.

All immunofluorescence experiments were done with at least 3 repeats, each repeat with a sample size of more than 10 individual flies.

Quantitative real-time PCR

Newly eclosed flies were placed in standard fly food for 4–7 days, and then, the same genotype flies were loaded into plastic tubes with OA-containing food or with standard fly food. After entraining for 2 days, flies were collected at the indicated time point (ZT8, local time 14:30), and total RNA was isolated from 40 heads using TRIzol Reagent (TIANGEN, #DP4-02). For reverse transcription and real-time PCR, we used PrimeScript™ RT reagent Kit with gDNA Eraser (Perfect Real Time; TakaRa, #RR047A) and SuperReal PreMix Plus (SYBR Green; TIANGEN, #FP205-02). All the experiments were performed using an Applied Biosystem StepOne Real-Time PCR system (Applied Biosystem, Foster, CA, U.S.). For qPCR quantification, *actin* was used as normalization control. The △△CT method was used for quantification. Student's *t*-test (Prism GraphPad) was used to compare the differences between genotypes. All primers used are listed in Table EV2. All quantitative RT–PCR experiments were done with 3 biological repeats, and sample size for each biological repeat was 30 fly heads. Three technical repeats were done for each biological repeat. All the *P*-values are listed in Table EV3.

Tissue-specific Dam-ID

Dam-ID plasmids were obtained From Andrea H Brand's laboratory (Marshall *et al*, 2016). *Pc* cDNA was cloned into the pUASTattB-LT3-Dam vector. The 3rd chromosome transgenic line was generated. The genotypes used for the final experiments were *stx*-Gal4/+; *Tub*-Gal80^{ts}/+; UAS-Dam/+ (GenoDam), *stx*-Gal4/+; *Tub*-Gal80^{ts}/+; UAS-*Pc*Dam/+ (Genocon) and *stx*-Gal4/+; *Tub*-Gal80^{ts}/UAS-*stx*flag; and UAS-*Pc*Dam/+ (Genoexp). For the experiments with *Tub*-Gal80^{ts}, flies were raised at 21° in LD cycle, the newly eclosed flies were heat shocked for 72 h at 29°C in an LD cycle, and the adult fly head tissues were collected and used for Dam-ID experiments. The details of the experimental protocol were described by Marshall *et al* (2016). The resulting DNA of the first round of PCR amplification was used as template for quantitative real-time PCR. All primers used are listed in Table EV2. A fold enrichment was calculated as follows:

$$\text{Fold enrichment} = 2^{(\text{CT GenoDam Primer} - \text{CT GenoDam PGRP-L}) - (\text{CT Genoexp Primer} - \text{CT Genoexp PGRP-L})}.$$

The sample size for each genotype was 50 flies per repeat. Three repeats were done for each experiment.

RNA-seq

Drosophila heads of *stx*^{d77} and control at ZT8 were used for RNA-seq. The RNA-seq was done by Biomics Company in Beijing, China (http://www.biomics.com.cn/), following standard protocols. Each sample contained 40 individual flies.

Data availability

The RNA-seq data from this publication have been deposited to the NCBI bioproject database https://www.ncbi.nlm.nih.gov/bioproject/ and assigned the identifier PRJNA513466 (https://www.ncbi.nlm.nih.gov/bioproject/?term = PRJNA513466).

Expanded View for this article is available online.

Acknowledgements
This work was supported by National Natural Science Foundation of China (Grant number 31772535) to Juan Du, National Natural Science Foundation of China (Grant number 31730076) to Zhangwu Zhao, and the National Natural Science Foundation of China (Grant number 31830058) to Alan J. Zhu. We would like to thank Dr. Jeffrey Price (University of Missouri at Kansas City, U. S.) for revision of this manuscript, Dr. Amita Sehgal (University of Pennsylvania, U. S.) for valuable discussions, and Dr. Andrea Brand (University of Cambridge, U.K.) for sharing the Dam-ID plasmids.

Author contributions
ZZ supervised all the data collecting process, analyzed the data and edited the manuscript. XZ performed the experiments, analyzed the data and edited the manuscript. TH, XW and PL performed a part of the experiments. AJZ provided the experimental materials and edited the manuscript. JD designed the study, analyzed data and wrote the manuscript.

Conflict of interest
The authors declare that they have no conflict of interest.

References

Aguilar-Arnal L, Sassone-Corsi P (2015) Chromatin landscape and circadian dynamics: Spatial and temporal organization of clock transcription. *Proc Natl Acad Sci USA* 112: 6863 – 6870

© 2021 The Authors

Busch S, Selcho M, Ito K, Tanimoto H (2009) A map of octopaminergic neurons in the *Drosophila* brain. *J Comp Neurol* 513: 643 – 667

Crocker A, Sehgal A (2008) Octopamine regulates sleep in *Drosophila* through protein kinase A-dependent mechanisms. *J Neurosci* 28: 9377 – 9385

Crocker A, Shahidullah M, Levitan IB, Sehgal A (2010) Identification of a neural circuit that underlies the effects of octopamine on sleep: wake behavior. *Neuron* 65: 670 – 681

Deng B, Li Q, Liu X, Cao Y, Li B, Qian Y, Xu R, Mao R, Zhou E, Zhang W *et al* (2019) Chemoconnectomics: mapping chemical transmission in *Drosophila*. *Neuron* 101: 876 – 893.e4

Doi M, Hirayama J, Sassone-Corsi P (2006) Circadian regulator CLOCK is a histone acetyltransferase. *Cell* 125: 497 – 508

Donlea JM, Thimgan MS, Suzuki Y, Gottschalk L, Shaw PJ (2011) Inducing sleep by remote control facilitates memory consolidation in *Drosophila*. *Science* 332: 1571 – 1576

Donlea JM, Ramanan N, Silverman N, Shaw PJ (2014) Genetic rescue of functional senescence in synaptic and behavioral plasticity. *Sleep* 37: 1427 – 1437

Donlea JM, Pimentel D, Talbot CB, Kempf A, Omoto JJ, Hartenstein V, Miesenböck G (2018) Recurrent circuitry for balancing sleep need and sleep. *Neuron* 97: 378 – 389.e4

Dubowy C, Sehgal A (2017) Circadian rhythms and sleep in *Drosophila melanogaster*. *Genetics* 205: 1373 – 1397

Du J, Zhang J, He T, Li Y, Su Y, Tie F, Liu M, Harte PJ, Zhu AJ (2016) Stuxnet facilitates the degradation of Polycomb protein during development. *Dev Cell* 37: 507 – 519

El-Brolosy MA, Kontarakis Z, Rossi A, Kuenne C, Günther S, Fukuda N, Kikhi K, Boezio GLM, Takacs CM, Lai SL *et al* (2019) Genetic compensation triggered by mutant mRNA degradation. *Nature* 568: 193 – 197

El-Kholy S, Stephano F, Li Y, Bhandari A, Fink C, Roeder T (2015) Expression analysis of octopamine and tyramine receptors in *Drosophila*. *Cell Tissue Res* 361: 669 – 684

Etchegaray JP, Lee C, Wade PA, Reppert SM (2003) Rhythmic histone acetylation underlies transcription in the mammalian circadian clock. *Nature* 421: 177 – 182

Etchegaray JP, Yang X, DeBruyne JP, Peters AH, Weaver DR, Jenuwein T, Reppert SM (2006) The polycomb group protein EZH2 is required for mammalian circadian clock function. *J Biol Chem* 281: 21209 – 21215

Fussnecker BL, Smith BH, Mustard JA (2006) Octopamine and tyramine influence the behavioral profile of locomotor activity in the honey bee (*Apis mellifera*). *J Insect Physiol* 52: 1083 – 1092

Gohl DM, Silies MA, Gao XJ, Bhalerao S, Luongo FJ, Lin CC, Potter CJ, Clandinin TR (2011) A versatile *in vivo* system for directed dissection of gene expression patterns. *Nat Methods* 8: 231 – 237

Hendricks JC, Finn SM, Panckeri KA, Chavkin J, Williams JA (2000) Rest in *Drosophila* is a sleep-like state. *Neuron* 25: 129 – 138

Liu Q, Liu S, Kodama L, Driscoll MR, Wu MN (2012) Two dopaminergic neurons signal to the dorsal fan-shaped body to promote wakefulness in *Drosophila*. *Curr Biol* 22: 2114 – 2123

Liu S, Liu Q, Tabuchi M, Wu MN (2016) Sleep drive is encoded by neural plastic changes in a dedicated circuit. *Cell* 165: 1347 – 1360

Ludin NM, Cheeseman JF, Merry AF, Millar CD, Warman GR (2016) The effects of the general anaesthetic isoflurane on the honey bee (*Apis mellifera*) circadian clock. *Chronobiol Int* 33: 128 – 133

Marshall OJ, Southall TD, Cheethamv SW, Brand AH (2016) Cell-type-specific profiling of protein-DNA interactions without cell isolation using targeted DamID with next-generation sequencing. *Nat Protoc* 11: 1586 – 1598

Ma Z, Zhu P, Shi H, Guo L, Zhang Q, Chen Y, Chen S, Zhang Z, Peng J, Chen J (2019) PTC-bearing mRNA elicits a genetic compensation response via Upf3a and COMPASS components. *Nature* 568: 259 – 263

McGuire SE, Le PT, Osborn AJ, Matsumoto K, Davis RL (2003) Spatiotemporal rescue of memory dysfunction in *Drosophila*. *Science* 302: 1765 – 1768

Müller J, Gaunt S, Lawrence PA (1995) Function of the Polycomb protein is conserved in mice and flies. *Development* 121: 2847 – 2852

Nakahata Y, Kaluzova M, Grimaldi B, Sahar S, Hirayama J, Chen D, Guarente LP, Sassone-Corsi P (2008) The NAD+-dependent deacetylase SIRT1 modulates CLOCK-mediated chromatin remodeling and circadian control. *Cell* 134: 329 – 340

Nicolaï LJ, Ramaekers A, Raemaekers T, Drozdzecki A, Mauss AS, Yan J, Landgraf M, Annaert W, Hassan BA (2010) Genetically encoded dendritic marker sheds light on neuronal connectivity in *Drosophila*. *Proc Natl Acad Sci USA* 107: 20553 – 20558

Pimentel D, Donlea JM, Talbot CB, Song SM, Thurston AJF, Miesenböck G (2016) Operation of a homeostatic sleep switch. *Nature* 536: pageFirst>333 – 337

Qi YX, Xu G, Gu GX, Mao F, Ye GY, Liu W, Huang J (2017) A new *Drosophila* octopamine receptor responds to serotonin. *Insect Biochem Mol Biol* 90: 61 – 70

Rosato E, Kyriacou CP (2006) Analysis of locomotor activity rhythms in Drosophila. *Nat Protoc* 1: 559 – 568

Rossi A, Kontarakis Z, Gerri C, Nolte H, Hölper S, Krüger M, Stainier DY (2015) Genetic compensation induced by deleterious mutations but not gene knockdowns. *Nature* 524: 230 – 233

Seidner G, Robinson JE, Wu M, Worden K, Masek P, Roberts SW, Keene AC, Joiner WJ (2015) Identification of neurons with a privileged role in sleep homeostasis in *Drosophila melanogaster*. *Curr Biol* 25: 2928 – 2938

Shaw PJ, Cirelli C, Greenspan RJ, Tononi G (2000) Correlates of sleep and waking in *Drosophila melanogaster*. *Science* 287: 1834 – 1837

Shaw PJ, Tononi G, Greenspan RJ, Robinson DF (2002) Stress response genes protect against lethal effects of sleep deprivation in *Drosophila*. *Nature* 417: 287 – 291

Southall TD, Gold KS, Egger B, Davidson CM, Caygill EE, Marshall OJ, Brand AH (2013) Cell-type-specific profiling of gene expression and chromatin binding without cell isolation: assaying RNA Pol II occupancy in neural stem cells. *Dev Cell* 26: 101 – 112

Sujkowski A, Ramesh D, Brockmann A, Wessells R (2017) Octopamine drives endurance exercise adaptations in *Drosophila*. *Cell Rep* 21: 1809 – 1823

Tamayo AG, Duong HA, Robles MS, Mann M, Weitz CJ (2015) Histone monoubiquitination by Clock-Bmal1 complex marks Per1 and Per2 genes for circadian feedback. *Nat Struct Mol Biol* 22: 759 – 766

Teng X, Dayhoff-Brannigan M, Cheng WC, Gilbert CE, Sing CN, Diny NL, Wheelan SJ, Dunham MJ, Boeke JD, Pineda FJ *et al* (2013) Genome-wide consequences of deleting any single gene. *Mol Cell* 52: 485 – 494

Valekunja UK, Edgar RS, Oklejewicz M, van der Horst GT, O'Neill JS, Tamanini F, Turner DJ, Reddy AB (2012) Histone methyltransferase MLL3 contributes to genome-scale circadian transcription. *Proc Natl Acad Sci USA* 110: 1554 – 1559

Vitaterna MH, Pinto LH, Takahashi JS (2006) Large-scale mutagenesis and phenotypic screens for the nervous system and behavior in mice. *Trends Neurosci* 29: 233 – 240

 © 2021 The Authors

Vu V, Verster AJ, Schertzberg M, Chuluunbaatar T, Spensley M, Pajkic D, Hart GT, Moffat J, Fraser AG (2015) Natural variation in gene expression modulates the severity of mutant phenotypes. *Cell* 162: 391 – 402

Weisel-Eichler A, Haspel G, Libersat F (1999) Venom of a parasitoid wasp induces prolonged grooming in the cockroach. *J Exp Biol* 202: 957 – 964

Xu Y, Guo W, Li P, Zhang Y, Zhao M, Fan Z, Zhao Z, Yan J (2016) Long-range chromosome interactions mediated by cohesin shape circadian gene expression. *PLoS Genet* 12: e1005992

Yellman C, Tao H, He B, Hirsh J (1997) Conserved and sexually dimorphic behavioral responses to biogenic amines in decapitated *Drosophila*. *Proc Natl Acad Sci USA* 94: 4131 – 4136

Young JM, Armstrong JD (2010) Structure of the adult central complex in *Drosophila*: organization of distinct neuronal subsets. *J Comp Neurol* 518: 1500 – 1524

Zhang YQ, Rodesch CK, Broadie K (2002) Living synaptic vesicle marker: synaptotagmin-GFP. *Genesis* 34: 142 – 145

© 2021 The Authors